Journal of Sol-Gel Science and Technology 1:177–184 (1994).

Sol-Gel ZrO_2 Coatings for Chemical Protection of Stainless Steel

PEDRO DE LIMA NETO, MOHAMED ATIK, LUIS A. AVACA, AND MICHEL A. AEGERTER
Institute of Physics and Chemistry of São Carlos, University of São Paulo, Cx. Postal 369, 13560-970-São Carlos (SP), Brazil

Abstract. ZrO_2 coatings deposited on 316 L stainless steel sheets were synthesized by sol-gel method using $Zr(OC_3H_7)_4$ as precursor and isopropanol, glacial acetic acid, and water as solvents for application with ultrasounds. Different solutions for dip-coating were prepared with compositions varying between 0.025 and 0.9 mol/dm^3 of ZrO_2. X-ray diffraction shows that the films densified at 800°C are crystalline with a tetragonal structure. The thickness of the coatings varied from 0.35-0.75 μm. The influence of the ZrO_2 coatings on the corrosion behavior of stainless steel substrates in aqueous NaCl was studied through potentiodynamic polarization curves at 1 mV/s. The values of the electrochemical parameters allow for an explanation of the role of the films in the increased resistance of steel against corrosion in moderately aggressive environments.

Key words: sol-gel coatings, chemical protection, stainless steel, ZrO_2, corrosion

1 Introduction

Sol-gel methods are now widely used for preparing inorganic materials from solutions containing metal compounds such as metal alkoxides, metal acetylacetonates, inorganic compounds, etc., with water as hydrolysing agent and alcohols as solvent [1, 2]. The fabrication of films via these methods offers potential advantages over traditional techniques such as low temperature processing, easy coating of large surfaces, easy adjustment of films thickness, high optical quality, low cost of processing infrastructure, large variety of deposition techniques (dip-, spin-, and spray-coating and electrophorese), etc. [3–5].

The chemical processing and the technical applications of sol-gel films have been recently reviewed by Schmidt [6] and Sakka and Yoko [7], respectively. A great variety of coating films have already been prepared by the sol-gel methods, and their properties have been used or proposed for various purposes which encompass applications in optical, electronic, optoelectronic, photonic, biotechnological, chemical, and mechanical fields.

The preparation and characterization of sol-gel films having specific *chemical functions* have been scarcely studied. Sol-gel films of TiO_2 [8, 9], $SrTiO_3$ [10], $BaTiO_3$ [10], α-Fe_2O_3 [11], and $NiFe_2O_4$ [12] compositions exhibit interesting photoelectrochemical properties as catalysts for hydrogen generation by decomposition of water. Al_2O_3:Pt [13]; TiO_2:Pd [14]; and SiO_2 (TiO_2 or Al_2O_3): Fe, Co, or Ni [15–17] are promising for catalysis application. The main efforts, however, have been realized in the field of chemical protection against acid and air corrosion, which cost millions of US dollars to society annually. Films such as Al_2O_3 [18], Si-O-N, and Si_3N_4 [19, 20] can be used for semiconductor passivation. SiO_2 is well known to prevent alkali diffusion and may be used as an intermediate coating between alkali glass and another functional coating [21] or to protect Si wafers [22]. TiO_2-CeO_2 [23, 24], SiO_2-TiO_2-ZrO_2 [25], and TiO_2-B_2O_3 [26] have been used to protect glasses, and SiO_2, SiO_2-Al_2O_3, TiO_2, and SiO_2-B_2O_3-Al_2O_3-BaO have been shown to offer good corrosion protection for Ag mirrors [27]. The prevention of chemical corrosion and oxidation of mild steel, carbon steel, and various types of stainless steel has been tested with SiO_2 [28], SiO_2-B_2O_3 [29, 30], mulite ($2SiO_2$-$3Al_2O_3$) [31], ZrO_2 [32–37], MTOS [38], and ZrO_2-CeO_2 [39]. All these coatings increase the protection of metal substrates from air ox-

idation (tested up to 800°C) and acid attack (tested up to 90°C).

The corrosion protection is strongly dependent on the thickness of the film and its structural quality. The presence of cracks and pores definitively degrades its efficiency. The most promising prevention for stainless steel so far has been reported by Atik, Aegerter, and Zarzycki using ZrO_2, TiO_2-SiO_2, SiO_2-Al_2O_3, and TiO_2-CeO_2 coatings [32, 33, 35, 40]. These coatings have been fabricated by a dip-coating technique using a sol preparation envolving sonocatalysis. The characterization performed by measuring the weight loss (H_2SO_4 corrosion) and weight gain (air oxidation) of small sheets (2×4 cm^2) has shown excellent results even at high temperature.

In this paper we present the results of a systematic electrochemical corrosion study of ZrO_2 films prepared by the same procedures and deposited on stainless steel 316 L, a material widely used for marine and chemical industry environments [41]. The corrosion characteristics of the samples, either bare stainless steel or coated with ZrO_2 of different thickness, were evaluated through potentiodynamic polarization curves obtained in aqueous NaCl solutions at room temperature and through analysis of the relevant electrochemical parameters.

2 Experimental

2.1 Substrate

The substrate used was 316 L stainless steel of composition (wt.%): 67.25 Fe, 18.55 Cr, 11.16 Ni, 2.01 Mo, 0.026 Cu, 0.15 Si, and 0.028 C. Samples ($3.0 \times 1.5 \times 0.1$ cm) were mechanically cut from large foils and then degreased ultrasonically in acetone.

2.2 Preparation of the Films

Zirconium propoxide $Zr(OC_3H_7)_4$ was used as source of zirconia. The sol was prepared by dissolving the alkoxide in isopropanol (C_3H_7OH), to which a small amounts of acetic acid (CH_3OOH) and excess water were added to complete the hydrolysis. The concentration of the starting alkoxide solutions varied between 0.025, and 0.9 mol/l ZrO_2. The volume ratios H_2O/C_3H_7OH and H_2O/CH_3COOH were 1 and 2, respectively. The mixture was submitted to ultrasonic irradiation (sonicator W 385 Heat Systems-Ultrasonics, Inc., 20 KHz). After 20 min, the liquid became homogeneous and transparent; the sols were found stable for up to four weeks at room temperature when kept in a closed vessel.

Dip-coated samples were prepared by withdrawing the substrates from the sonosolutions at a constant rate of 10 cm/min. The resulting gel films were dried at 40°C for 15 minutes and then thermally treated at a rate of 5°C/min with two isothermal holdings, the first at 400°C for 1 hour and the second at 800°C for 2 hours.

The thickness of ZrO_2 coatings after heat treatment in air at 800°C for 2 hours varied beween 0.35 μm and 0.75 μm, depending on the sol concentration. ZrO_2 coated substrates sintered at that temperature with films having a thickness ≥ 0.67 μm presented cracks. However, ZrO_2 coatings thinner than 0.5 μm were found continuous and visually crack free. For the present work, samples having film thicknesses of 0.5 μm and 0.7 μm were used, and their electrochemical behavior was compared to that of bare 316 L stainless steel plates.

2.3 Characterization of the Films

Analysis of coated substrates was made by using a Rigaku Rotaflex diffractometer with a characteristic CuK_α radiation. X-ray diffraction data confirmed that the films densified at 800°C have the tetragonal ZrO_2 structure (111 peak at d = 2.98 Å). A FTIR spectrometer with a 400–4000 cm^{-1} range was used to obtain high resolution spectra of coatings; the measurements were performed by reflection at an incident angle of 30°. Unsintered samples show characteristic OH bands at ~3600 cm^{-1}, Zr-O-C groups at 1476.8 cm^{-1} and 1452.8 cm^{-1}, and Zr-O-Zr at 665.7 cm^{-1}. During sintering, the OH and Zr-O-C bands disappear and the Zr-O-Zr band increases strongly. Details of these analyses can be found elsewhere [32].

2.4 Electrochemical Measurements

A very convenient and precise way of evaluating the corrosion behavior of a material in a given medium is the recording of the complete polarization curve under potentiostatic control [42]. Thus, starting at the cathodic end, the electrode potential is anodically shifted in a continuous and slow fashion (e.g., 1 mV/s) until the (anodic) current reaches a pre-established maximum value. By means of appropriate software, it is possible to determine the Tafel slope for both cathodic and anodic processes. Linear least-squares fitting of the experimental data to the Stern-Geary equation [42] determines the point at which the anodic and cathodic current densities are equal in magnitude, thus yielding a zero net current. This point defines the corrosion potential (E_{corr}) as well as the corrosion current density (i_{corr}).

The software also gives the polarization resistance (R_p) of the system. This last value is obtained by analysis of the linear response i vs. E close to the corrosion potential, which in turn can also be determined using Tafel slopes [42]. For actively dissolving metals, the two values of E_{corr} described above must coincide, whereas this is not the case when the anodic branch of the polarization curve shows a region of passive or quasi-passive behavior. In the later case, the meaningful value of E_{corr} is that measured at $i \approx 0$ and not the one obtained by extrapolation of the Tafel lines. Finally, the calculations also furnish the corrosion rate (C.R.), which is a measure in mils per year (MPY) of the amount of metal being dissolved in the medium under consideration.

A comparison of E_{corr} values for different materials in the same medium allows one to establish the relative stability of those materials with regard to corrosion. The more anodic the value of E_{corr}, the higher the corrosion resistance of the sample. A similar analysis could be done using the values of the corrosion current; in this case, however, it is necessary to be sure that the cathodic reaction (either hydrogen evolution or oxygen reduction) remains unchanged between experiments, since i_{corr} is much more sensitive than E_{corr} to small changes in the cathodic branch of the polarization curve.

In the present work, the electrochemical measurements were performed using a PAR Model 273 Potentiostat/Galvanostat linked to a microcomputer for data acquisition and handling through the PAR Model 342 Corrosion Measurement Software. The experiments were carried out at room temperature in air-saturated aqueous NaCl solutions of various concentrations. The working electrodes employed were 316 L stainless steel plates, either bare or coated with ZrO_2 of 0.5 μm and 0.7 μm thickness, respectively, immersed 1 cm into the solution. A Pt-foil was the secondary electrode while the reference electrode was of the saturated calomel type (SCE).

3 Results and Discussion

Figures 1–3 show the complete polarization curves obtained for the three samples under investigation in aqueous NaCl solutions with concentrations 100, 200, and 300 g/dm^3, respectively. The curves were recorded a few minutes after immersion of the samples in order to allow stabilization of the system. Some experiments were also performed using 30 g/dm^3 NaCl, which simply confirmed the trends observed with other solutions. In all cases, the cathodic branch of the curves shows a tendency towards a plateau, probably due to a limiting current controlled by O_2 diffusion in the NaCl solutions. In contrast, the anodic branch of the curves changes drastically in the presence of the coatings. The observed effects do not follow a logical sequence with the electrolyte concentration and/or the ZrO_2 film thickness, but in most cases the quasi-passive region shown by the bare 316 L stainless steel is disrupted. This is a indication that the pitting of the surface is altered in the presence of the films [42]. Meanwhile, the most marked effect of the coatings on the corrosion behavior of 316 L stainless steel is the shift of the corrosion potential towards more noble values. This shift, that in some cases amounts to ~300 mV (figure 2), is a clear indication of the protective properties of the films with regard to the corrosion of stainless steel in

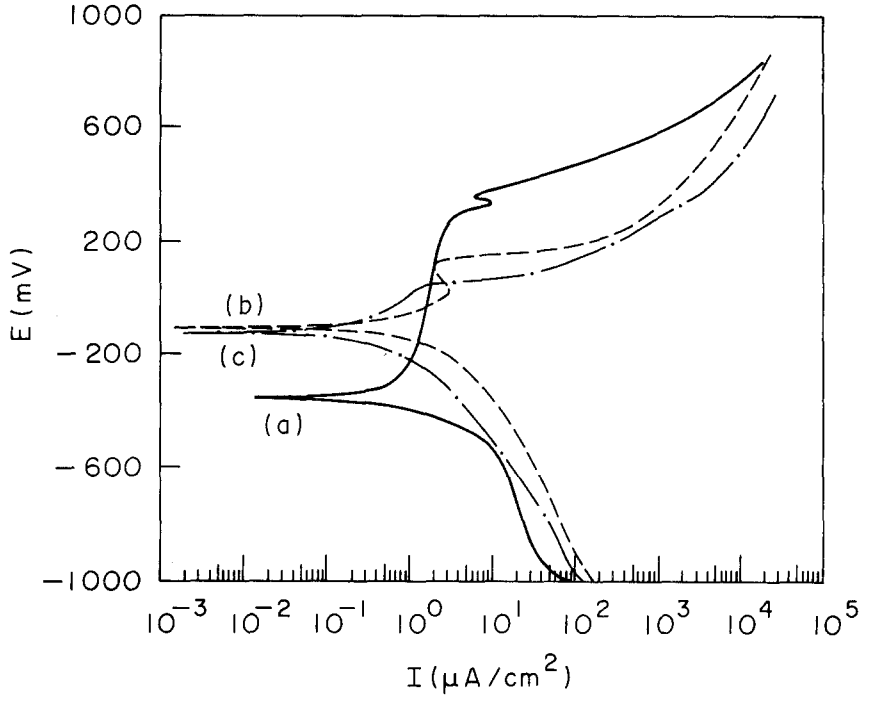

Fig. 1. Polarization curves recorded at 1 mV/s in aqueous NaCl, 100 g/dm^3 at room temperature for: (a) bare 316 L stainless steel, (b) coated with ZrO_2 (0.5 μm), and (c) coated with ZrO_2 (0.7 μm). Potentials referred to SCE.

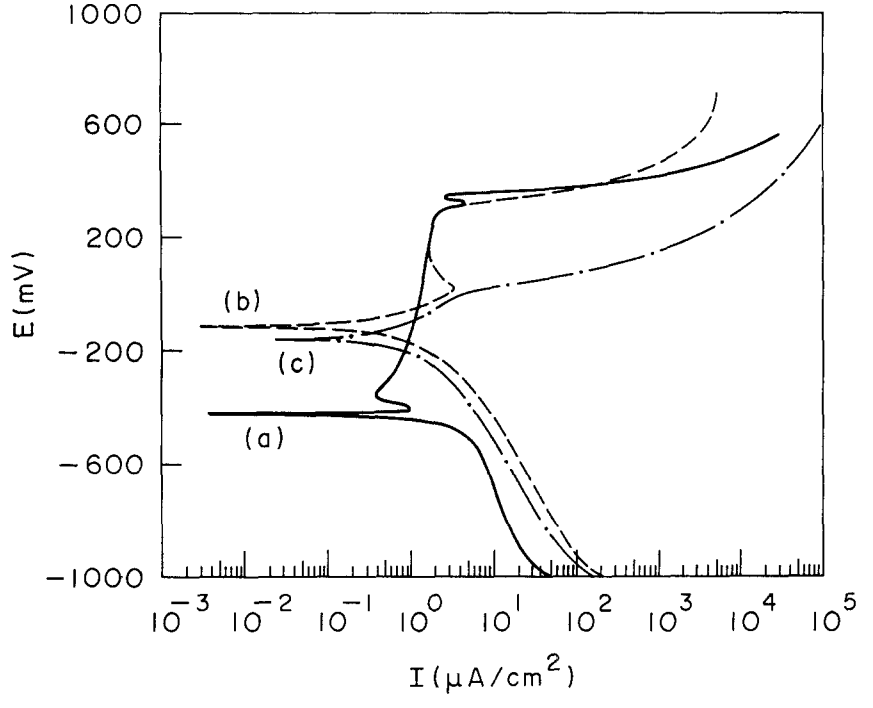

Fig. 2. Same as Fig. 1, but for aqueous NaCl, 200 g/dm^3 solution.

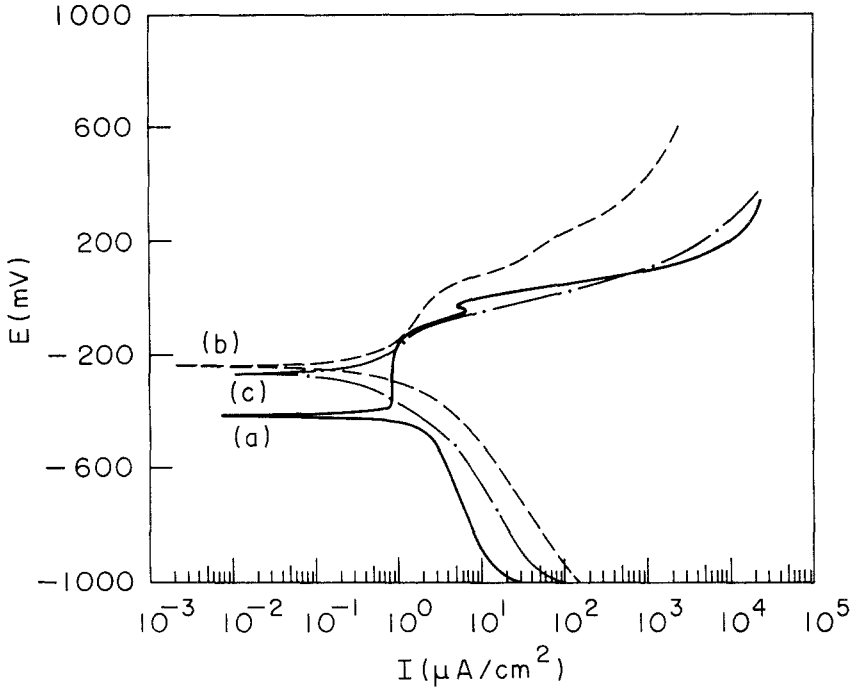

Fig. 3. Same as Fig. 1, but for acqueous NaCl, 300 g/dm^3 solution.

NaCl solutions.

Tables 1–3 collect the electrochemical parameters obtained from the polarization curves by means of the corrosion software employed. In all cases, the experiments were repeated several times, and the results reported for bare 316 L stainless steel and ZrO_2 (0.5 μm) coatings correspond to mean values of at least three independent measurements which showed small variation (e.g., ± 5 mV for E_{corr}). In the case of ZrO_2 (0.7 μm) coatings, the results were not reproducible from sample to sample; some extreme results are presented in Tables 1 and 2. Moreover, the correlation between the different parameters measured was not logical, indicating that the system under study was not properly defined. This must be a consequence of the cracks present in the coating.

Disregarding the results obtained for ZrO_2 (0.7 μm) coatings for the reason given above, Tables 1-3 show that the ZrO_2 (0.5 μm) coatings have a profound effect on the corrosion behavior of 316 L stainless steel in aqueous NaCl solutions. First, the corrosion potential is shifted in the anodic direction by up to 300 mV, making the material more resistant to the attacks by the medium. Second, the value of the corrosion current shows large variations from experiment to experiment, dropping by a factor of 17 in one of the cases (Table 2). The combination of these results (E_{corr} and i_{corr}) suggest that the bare material with the ZrO_2 coating will have a much longer useful life than without it. Meanwhile, experiments carried out using bare 316 L stainless steel plates heat-treated at 800°C for 2 hours showed that this procedure also alters the corrosion behavior of the steel, raising some doubts in relation to the material to which the comparisons should be made. To overcome this problem, efforts are being made to found conditions and appropriate additives that could allow lower temperatures in the densification steps of the ZrO_2 coatings.

Comparison of the data at different NaCl concentrations is somewhat difficult since the solutions were air-saturated, meaning that O_2 concentration will be lower for the more concentrated chloride solutions [42]. Nevertheless,

Table 1. Electrochemical corrosion parameters derived from the polarization curves obtained at room temperature with an aqueous NaCl (100 g/dm^3 test solution). E_{corr}: corrosion potential (mV vs. SCE), i_{corr}: corrosion current (μA/cm^2), R_p: polarization resistance (kΩ cm^2), C.R.: corrosion rate (mils per year, MPY).

Sample	$-E_{corr}$ (mV vs. SCE)	i_{corr} (μA/cm^2)	R_p (kΩ cm^2)	C.R. (MPY)
316 L stainless steel	339	0.48	62.6	0.26
ZrO_2 (0.5 μm)	98	0.35	167.7	0.16
ZrO_2 (0.7 μm)	112	0.20	384.8	0.09
	152	0.08	585.1	0.04

Table 2. Same as in Table 1, but for aqueous NaCl (200 g/dm^3) test solution.

Sample	$-E_{corr}$ (mV vs. SCE)	i_{corr} (μA/cm^2)	R_p (kΩ cm^2)	C.R. (MPY)
316 L stainless steel	418	4.85	18.8	2.27
ZrO_2 (0.5 μm)	110	0.28	194.1	0.13
ZrO_2 (0.7 μm)	295	0.80	144.3	0.37
	162	0.55	121.0	0.26

Table 3. Same as in Table 1, but for aqueous NaCl (300 g/dm^3) test solution.

Sample	$-E_{corr}$ (mV vs. SCE)	i_{corr} (μA/cm^2)	R_p (kΩ cm^2)	C.R. (MPY)
316 L stainless steel	415	2.21	14.3	1.04
ZrO_2 (0.5 μm)	225	0.40	215.0	0.19
ZrO_2 (0.7 μm)	260	0.31	90.0	0.14

when the NaCl concentration increases, two apparently contradictory effects can be observed. The corrosion potentials move cathodically, but the corrosion currents (or rates) go through a maximum for the bare plates and through a minimum for the ZrO_2 (0.5 μm) coatings. This must be a combination of the increment in chloride concentration, which makes the medium more aggressive, and the simultaneous depletion in O_2 concentration, which decreases the rate of the prevailing cathodic reaction under these conditions. It also indicates that the electrochemical reactions occurring on both types of materials should be different; a detailed knowledge of this will require further studies. Apart from those effects, the overall results indicate once again that the ZrO_2 coatings has an efficient protective role against the corrosion of 316 L stainless steel.

These findings qualitatively confirm previous observations [32, 33], where the corrosion behavior of similar samples was measured through weight gains in air and weight losses in 15% H_2SO_4 at elevated temperatures. However, the electrochemical techniques employed here are much more sensitive than the previous ones, and useful quantitative information can be obtained in short times.

4 Conclusion

With a single dip-coating procedure, crystalline films of ZrO_2 with a tetragonal structure can be produced on 316 L stainless steel sheets. The results show that ZrO_2 coatings of about 0.5 μm in thickness provide an effective corrosion protection of these metal substrates in aqueous NaCl solutions. Thicker films present cracks after air densification at 800°C and are less protective.

Acknowledgments

This research was sponsored by FAPESP, FINEP, CNPq, CAPES/PICD, and the Program RHAE-Novos Materiais (Brazil).

References

1. C.J. Brinker and G.W. Scherer, *Sol-Gel Science: the Physics and Chemistry of Sol-Gel Processing* (Academic Press, San Diego, 1990).
2. M.A. Aegerter, M. Jafelicci Jr., D.F. Souza, and E.D. Zanotto, ed., *Sol-Gel Science and Technology* (World Scientific, Singapore, 1991).
3. H. Dislich, in *Sol-Gel Technology for Thin Films, Preforms, Electronics, and Specialty Shapes*, edited by L.C. Klein (Noyes Publications, Park Ridge, 1988), p. 50.
4. R.B. Pettit, C.S. Ashley, S.T. Reed, and C.J. Brinker, in *Sol-Gel Technology for Thin Films, Preforms, Electronics, and Specialty*, edited by L.C. Klein (Noyes Publications, Park Ridge, 1988), p. 80.
5. S. Sakka, Reference 2, p. 346.
6. H. Schmidt, in *Chemistry, Spectroscopy and Applications of Sol-Gel Glasses*, edited by R. Reisfeld and C.K. Jorgensen (Springer-Verlag, Berlin, 1992), p. 119.
7. S. Sakka and T. Yoko, in *Chemistry, Spectroscopy and Applications of Sol-Gel Glasses*, edited by R. Reisfeld and C.K. Jorgensen (Springer-Verlag, Berlin, 1992), p. 90.
8. T. Yoko, K. Kamiya, A. Yuasa, K. Tanaka, and S. Sakka, J. Non-Cryst. Solids **100**, 483 (1988).
9. T. Yoko, A. Yuasa, K. Kamiya, and S. Sakka, J. Electrochem. Soc. **138** 8, (1991).
10. T. Yoko, A. Yuasa, K. Kamiya, K. Tanaka, and S. Sakka, Res. Rep. Fac. Eng. Mie Univ. **12**, 41 (1987).
11. T. Yoko, K. Kamiya, K. Tanaka, and S. Sakka, Res. Rep. Bull. Chem. Res. Kyoto Univ. **67**, 249 (1990).
12. T. Yoko, Y. Inagaki, and S. Sakka, Rep. Asahi Glass Foundation Ind. Techn. **13**, 56 (1990).
13. J.D. Cairns, D.L. Segal, and J.L. Woodhead, Mat. Res. Soc. Symp. **32**, 135 (1984).
14. G. Carturan, G. Facchin, G. Navaziv, V. Gottardi, and G. Cocco, in *Ultrastructure Processing of Ceramics, Glasses and Composites*, edited by L.L. Hench and D.R. Ulrich (J. Wiley, New York, 1984), p. 197.
15. A. Ueno, H. Suzuki, and Y. Kotera, J. Chem. Soc. Faraday Trans. **179**, 127 (1983).
16. T. Ida, H. Tsuihi, A. Ueno, K. Tohki, Y. Udaga, K. Imai, and T. Sano, J. Catal. **106**, 428 (1987).
17. S. Sakka, Catalysts **32**, 2 (1990) (in Japanese).
18. J. Schlichting and S. Neumann, J. Non-Cryst. Solids **48**, 185 (1982).
19. J. Martinsen, R.A. Figat, and M.W. Shafer, Mat. Res. Soc. Symp. Proc. **32**, 361 (1984).
20. R.K. Brow and C.G. Pantano, Mat. Res. Soc. Symp. Proc. **32**, 361 (1982).
21. S. Ogiwara and K. Kinugawa, Yogyo-Kyokai-Shi **90**, 157 (1982) (in Japanese).
22. P.M. Glaser and C.G. Pantano, J. Non-Cryst. Solids **63**, 209 (1984).
23. A. Makishima, H. Kubo, K. Wada, Y. Kitami, and T. Shimohira, J. Am. Ceram. Soc. **69**, C127 (1986).
24. A. Makishima, M. Asami, and K. Wada, J. Non-Cryst. Solids **121**, 310 (1990).
25. W. Beier, A.A. Göktas, and G.H. Frischat, J. Non-Cryst. Solids **100**, 531 (1988).
26. C.W. Hsieh, A.S.T. Chiang, C.C. Lee, and S.J. Yang, J. Non-Cryst. Solids **144**, 53 (1992).
27. S. Reed and C. Ashley, Mat. Res. Soc. Symp. Proc. **121**, 631 (1988).

28. O. de Sanctis, L. Gomez, N. Pelligri, C. Parodi, A. Marajofsky, and A. Duran, J. Non-Cryst. Solids **121**, 338 (1990).
29. N. Tohge, A. Matsuda, and T. Minami, Chem. Express **2**, 141 (1987).
30. M. Guglielmi, D. Festa, P.C. Innocenzi, P. Colombo, and M. Gobain, in *Proc. Sixth International Workshop on Glasses and Ceramics from Gels,* Seville 1991, J. Non Cryst. Solids **147–148**, 474–477 (1992).
31. A.R. Di Giampaolo, M. Puerta, J. Lira, and N. Ruiz, in *Proc. Sixth International Workshop on Glasses and Ceramics from Gels*, Seville 1991, J. Non Cryst. Solids **147–148**, 467–473 (1992).
32. M. Atik and M.A. Aegerter, in *Proc. Sixth International Workshop on Glasses and Ceramics from Gels*, Seville 1991, J. Non-Cryst. Solids **147–148**, 813–819 (1992).
33. M. Atik and J. Zarzycki, J. Mat. Sci. Lett., Accepted for publication.
34. A. Tomasi, P. Scardi and F. Marchetti, Mat. Res. Soc. Symp. Proc. **271**, 477–483 (1992).
35. M. Atik and M.A. Aegerter, Mat. Res. Soc. Symp. Proc. **271**, 471–476 (1992).
36. D. Ganguli and D. Kundu, J. Mat. Sci. Lett. **3**, 503 (1984).
37. N. Tohge, A. Matsuda, and T. Minami, *J. Am. Ceram. Soc.* **70**, C13 (1987).
38. K. Izumi, H. Tanaka, Y. Uchida, N. Tohge, and T. Minami, in *Proc. Sixth International Workshop on Glasses and Ceramics from Gels,* Seville 1991, J. Non Cryst. Solids **147–148**, 483–487 (1992).
39. R. di Maggio, P. Scardi, and A. Tomasi, Mat. Res. Soc. Symp. **180**, 481 (1990).
40. M. Atik and J. Zarzycki (to be published).
41. A.J. Sedriks, *Corrosion of Stainless Steels* (John Wiley & Sons, New York, 1979).
42. H.H. Uhlig and R.W. Revie, *Corrosion and Corrosion Control*, 3rd. Edition (John Wiley & Sons, New York, 1985).